

On-line Viewpoint and Motion Planning for Efficient Visual Navigation under Uncertainty

Inhyuk Moon¹, Jun Miura, and Yoshiaki Shirai

*Dept. of Computer-Controlled Mechanical Systems, Osaka University, Suita, Osaka
565-0871, Japan*

Received February 11, 1999

Abstract

This paper proposes an on-line viewpoint planning method for a mobile robot to reach a goal position safely *and* quickly. When a robot passes through a narrow space, it moves slowly while carefully observing surrounding objects and estimating the distances to the objects precisely. On the other hand, the robot moves quickly in a widely open space. To realize such a behavior of the robot, by considering both the predicted positional uncertainty and the configuration of obstacles, the viewpoint is adaptively determined according to the narrowness of the nearby environment. The planner works on-line to cope with actual errors. The robot motion is continuously performed with speed control between the planned viewpoints during visual processing. An experimental result using a mobile robot with stereo vision shows the validity of the proposed method.

Key words: Viewpoint planning, On-line planning, Uncertainty, Mobile robot, Stereo vision

¹ Corresponding author.; e-mail:ihmoon@cv.mech.eng.osaka-u.ac.jp

1 Introduction

It is an important function for an autonomous mobile robot to plan where to go and what to look based on the current information of the environment. Since sensing and motion usually includes uncertainty, the planner should take it into account[1]. In this paper, we propose an on-line viewpoint and motion planning method for a vision-based mobile robot to reach a goal position safely and quickly under uncertainty.

When a robot moves by dead reckoning, the positional uncertainty is increased by motion uncertainties such as control error or slippage. This uncertainty can be reduced by observing known landmarks using vision. However, the visual information includes uncertainty caused by quantization or calibration errors. In addition, visual processing requires much computation time.

Selection of viewpoints affects safety and efficiency of navigation strongly. If the robot reduces the number of observation to move fast, it will be dangerous due to the cumulative motion uncertainty. On the other hand, if the robot performs many observations, it can move safely, but will be late for arriving at the goal position[2].

There have been many works to cope with uncertainty. Ayache and Faugeras[3] formulated the integration of multiple sensory data with uncertainty. They considered the uncertainties of motion and vision, and estimated the state and the uncertainty of the robot using the Extended Kalman Filter. Kriegman et al.[4] realized a corridor navigation by exploring free spaces based on the map built from visual data with uncertainty. These studies concentrated on how to cope with the uncertainty, but did not consider how to determine viewpoints.

To solve the problem of high computational cost of visual processing, non-stop navigation methods were proposed[5,6]. The robot moves without stopping while processing the visual data; when it obtains the processing result later, it retroactively integrates the delayed sensory information into the state estimation. They, however, did not deal with the problem of what to look.

There are several works which deal with viewpoints

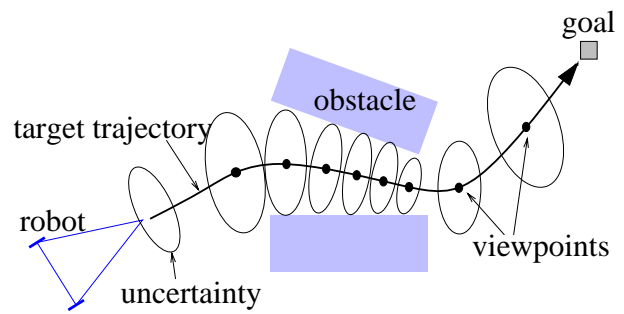


Fig. 1. Adaptive viewpoint selection with consideration of uncertainty; the line and ellipses indicate the target trajectory and positional uncertainties, respectively.

and landmark planning for mobile robots. Komoriya et al.[7] proposed a landmark planning method. The robot selects a landmark which minimizes the estimated uncertainty from landmark candidates. Since the viewpoint and landmarks are selected only when the positional uncertainty exceeds a pre-defined threshold, the resultant navigation may be inefficient. Nagatani and Yuta[8] proposed a method of planning paths and sensing points of the robot. They defined a cost function which consists of observation cost and collision risk of the robot. Candidates of the sensing points are given beforehand, and then the sensing points are determined so that the cost function is minimized. Since the candidates for the sensing points and the cost function are heuristically determined, it cannot be guaranteed that the planning result is efficient. Furthermore, the method does not take into account actual errors since the plan is generated offline.

In this paper, we propose an on-line viewpoint and motion planning method for safe and efficient navigation. Based on the uncertainty model of the motion and the observation, the robot selects viewpoints adaptively according to the nearby environment. Fig. 1 illustrates the idea of adaptive viewpoint selection with consideration of uncertainty. In a narrow space, the robot moves slowly and observes many times to reduce the uncertainty whereas it moves fast in a wide open space. This planning is performed on-line so that the robot can cope with actual errors.

This paper deals with a planning in a known indoor environment, where a complete map of objects and landmark candidates are given. The basic strategy of viewpoint planning is that the robot repeatedly se-

lects the farthest position which is guaranteed to be safe considering the uncertainty of the robot and the configuration of obstacles. As a result, distances between planned viewpoints are not uniform as shown in Fig. 1; the robot changes its speed at every viewpoint interval in order to move continuously without stopping. Experimental results using an actual mobile robot show the validity of the proposed method.

2 Modeling of uncertainty

Fig. 2 shows our 3-wheeled mobile robot which has a front steering wheel and two rear driving wheels. The stereo cameras are mounted on a mobile platform which can turn around the pan axis to control the viewing direction. The pan axis is located on the position of the front wheel.

2.1 Motion uncertainty

The state of the robot, $\mathbf{X} = [x \ y \ \theta \ \phi]^T$, consists of the position of the front wheel, (x, y) , the orientation of the robot, θ , and the viewing direction ϕ . Fig. 3 shows the motion model of the robot controlled by input $\mathbf{U} = [s \ \lambda \ \psi]^T$ which consists of a moving distance, a steering angle, and a pan angle. When the robot is controlled by angle λ , the center and the radius of the circular trajectory are determined. Then

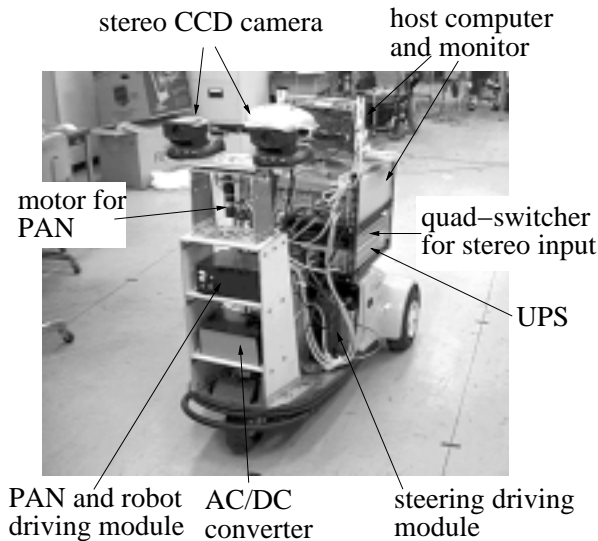


Fig. 2. The mobile robot.

the rotation angle of the robot, ζ_t , is calculated from s as $\zeta_t = (s_t \sin \lambda_t)/d$. The viewing direction ϕ is controlled by ψ . The state transition of the robot can be expressed by the following nonlinear equation:

$$\mathbf{X}_{t+1} = \begin{bmatrix} x_t + \frac{d}{\sin \lambda_t} \{\sin(\theta_t + \lambda_t + \zeta_t) - \sin(\theta_t + \lambda_t)\} \\ y_t + \frac{-d}{\sin \lambda_t} \{\cos(\theta_t + \lambda_t + \zeta_t) - \cos(\theta_t + \lambda_t)\} \\ \theta_t + \zeta_t \\ \phi_t + \psi_t \end{bmatrix} = \mathbf{F}(\mathbf{X}_t, \mathbf{U}_t). \quad (1)$$

If $\lambda_t \simeq 0$, Eq. (1) can be approximated using relation $\sin \lambda_t \approx \lambda_t$.

To predict the uncertainty of \mathbf{X}_{t+1} , we first derive the following linearized equation of Eq. (1) by the first-order Taylor series expansion around the mean values, $\hat{\mathbf{X}}_t$ and $\hat{\mathbf{U}}_t$:

$$\mathbf{X}_{t+1} \approx \mathbf{F}(\hat{\mathbf{X}}_t, \hat{\mathbf{U}}_t) + \frac{\partial \mathbf{F}}{\partial \mathbf{X}_t} (\mathbf{X}_t - \hat{\mathbf{X}}_t) + \frac{\partial \mathbf{F}}{\partial \mathbf{U}_t} (\mathbf{U}_t - \hat{\mathbf{U}}_t), \quad (2)$$

where the partial differentiation means Jacobian matrix at the mean value. The mean $\hat{\mathbf{X}}_{t+1}$ of the predicted state is equal to $\mathbf{F}(\hat{\mathbf{X}}_t, \hat{\mathbf{U}}_t)$. Thus, the covariance matrix of the predicted state error, Σ_{t+1} , can be obtained as follows:

$$\Sigma_{t+1} = E[(\mathbf{X}_{t+1} - \hat{\mathbf{X}}_{t+1})(\mathbf{X}_{t+1} - \hat{\mathbf{X}}_{t+1})^T]$$

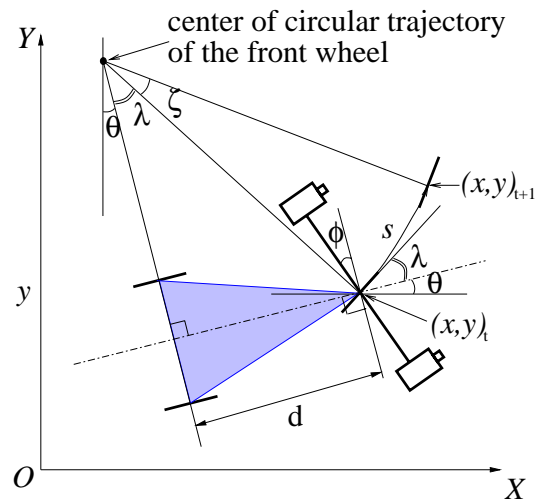


Fig. 3. Motion model of the front-steering mobile robot.

$$= \frac{\partial \mathbf{F}}{\partial \mathbf{X}_t} \Sigma_t \frac{\partial \mathbf{F}^T}{\partial \mathbf{X}_t} + \frac{\partial \mathbf{F}}{\partial \mathbf{U}_t} \Sigma_t \frac{\partial \mathbf{F}^T}{\partial \mathbf{U}_t}, \quad (3)$$

where Σ_t is the covariance matrix of the control input. Assuming that the control errors are Gaussian and independent of each other, Σ_t is expressed as a diagonal matrix form:

$$\Sigma_t = \begin{bmatrix} \sigma_s^2 & 0 & 0 \\ 0 & \sigma_\lambda^2 & 0 \\ 0 & 0 & \sigma_\psi^2 \end{bmatrix}, \quad (4)$$

where σ_s^2 denotes the variance of the odometry measurement error due to slippage, which is considered to be proportional to the distance input s ; σ_λ^2 and σ_ψ^2 are the variance of control input λ and ψ , respectively, which are constant. We experimentally found the errors are reasonably approximated by Gaussian. The variance of each error is determined from experimental results.

In this paper, we define the uncertainty area as the so-called 3σ ellipsoid obtained from Σ . The positional uncertainty of the robot is represented as an ellipse generated by projecting the ellipsoid on the X - Y plane. The boundary of the ellipse is an equiprobability contour. The uncertainty ellipse is obtained by $\mathbf{X}^T \Sigma^{-1} \mathbf{X} = 3^2$, where \mathbf{X} denotes a position (x, y) of the state \mathbf{X} , and Σ means the x - y components of the covariance matrix Σ .

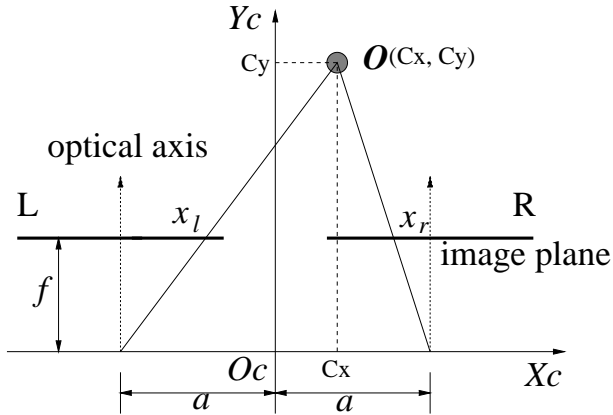


Fig. 4. Stereo geometry.

2.2 Observation uncertainty

The robot detects vertical segments as landmarks and calculates the position of a landmark in the camera coordinates using stereo geometry. Fig. 4 shows the geometry of stereo observation of a landmark located at $\mathbf{O} = [c_x \ c_y]^T$ on the X_c - Y_c plane. When the landmark is projected on $\mathbf{I} = [x_l \ x_r]^T$, which is the horizontal position in the stereo images, landmark position \mathbf{O} is represented as

$$\mathbf{O} = \mathbf{Z}(\mathbf{I}) = \begin{bmatrix} \frac{a(x_l + x_r)}{x_l - x_r} \\ \frac{2af}{x_l - x_r} \end{bmatrix}, \quad (5)$$

where f and $2a$ denote the focal length and the distance between the two cameras, respectively. Projected position \mathbf{I} includes an error caused by image quantization. Since the errors of x_l and x_r can be modeled as Gaussian and independent of each other[1], the covariance matrix of the projected position, Σ , is

$$\Sigma = \begin{bmatrix} \sigma_{x_l}^2 & 0 \\ 0 & \sigma_{x_r}^2 \end{bmatrix}. \quad (6)$$

The uncertainty of landmark position is obtained in the same manner as [4]. Using the Taylor series expansion around mean $\hat{\mathbf{I}}$, the linearized equation of Eq. (5) is obtained as follows:

$$\mathbf{O} \approx \mathbf{Z}(\hat{\mathbf{I}}) + \frac{\partial \mathbf{Z}}{\partial \mathbf{I}} (\mathbf{I} - \hat{\mathbf{I}}). \quad (7)$$

From Eq. (7), the positional uncertainty Σ is

$$\Sigma = \frac{\partial \mathbf{Z}}{\partial \mathbf{I}} \Sigma \frac{\partial \mathbf{Z}^T}{\partial \mathbf{I}}. \quad (8)$$

2.3 Utilizing observation information

Fig. 5 shows the geometry when the robot observes a landmark located at $\mathbf{L} = [L_x \ L_y]^T$ in the world coordinates. This relation can be expressed as follows:

$$\mathbf{L} = \mathbf{R}_{[(\theta+\phi)-\frac{\pi}{2}]} \mathbf{O} + \mathbf{X}, \quad (9)$$

where $\mathbf{R}_{[\rho]}$ denotes the rotation matrix with angle ρ . Eq. (9) can be rewritten in the following form:

$$G(\mathbf{X}_t, \mathbf{O}_t, L) = 0. \quad (10)$$

We can obtain a linearized observation equation of Eq. (10) using the Taylor series expansion. Utilizing the linearized equation, we can estimate the state and the uncertainty of the robot using the Extended Kalman Filter[3] (see Appendix A for details).

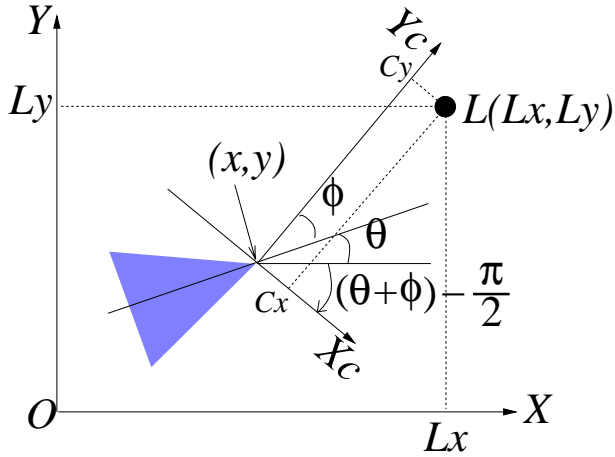


Fig. 5. Observation geometry.

3 Planning considering uncertainty

In this paper, we deal with planning of trajectory, viewpoint, motion, and landmark. First, we perform an off-line planning of the target trajectory from a given map. Then viewpoints and the control input at each viewpoint are determined on-line by considering uncertainty. Landmarks are selected considering their visibility and distance from the robot.

3.1 Planning of the target trajectory

Based on a given map, the robot plans the target trajectory off-line. First, it generates *obstacle regions* and *enlarged obstacle regions*. An obstacle region is obtained by enlarging an obstacle by the half width of the robot. If the robot touches an obstacle region, it is considered to collide with the obstacle. An enlarged obstacle region is obtained by adding the *safety*

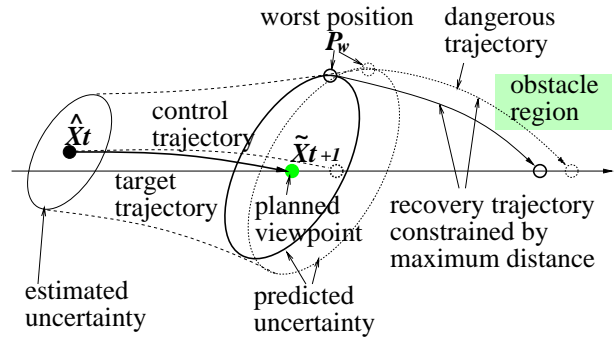


Fig. 6. On-line viewpoint planning strategy.

margin to the obstacle region, where the safety margin is determined as the maximum deviation from trajectory when the robot moves by a pre-defined maximum distance s_{max} between viewpoints. If two enlarged obstacle regions overlap, the overlapped area is classified as a *narrow space*; other areas are *open*. In a narrow space, the trajectory is generated so that the distances from the trajectory to the obstacles on both sides are roughly equal. In an open space, the robot determines the minimum-length trajectory which does not enter any enlarged obstacle regions. The planned target trajectory is composed of straight-line and circular segments, which are connected smoothly[2].

3.2 On-line viewpoint and motion planning

3.2.1 The worst position

We introduce the notion of *worst position* in order to check the safety of a viewpoint considering uncertainty. When the robot is controlled by an input U , it can predict the positional uncertainty at the next viewpoint from Eq. (3). The worst position P is defined as the most distant point from the target trajectory. We assume that all positions inside the uncertainty ellipse are safe if P is safe. Here, the safety means that P is not inside any obstacle region and the robot at P can recover to the target trajectory without collision. The robot checks the safety of the two worst positions on both side of the trajectory.

3.2.2 Determining viewpoint and motion

In order to reduce the number of observations as much as possible, the next viewpoint is determined to be the farthest *safe* position on the target trajectory from

the current position. Fig. 6 shows the proposed viewpoint planning method; a brief description of the method is as follows:

- (1) Set the initial input distance s_t to s_{max} .
- (2) Calculate a viewpoint on the target trajectory so that the distance of the recovery trajectory from the current position \hat{X}_t to the viewpoint becomes s_t . As a result, the steering control input λ_t is determined, and then the positional uncertainty of the robot at the calculated viewpoint, Σ_{t+1} , can be obtained. If the worst position P at the viewpoint is inside an obstacle region, decrease s_t by a certain value and go to (2). Otherwise, go to (3).
- (3) Calculate the recovery trajectory from P to the target trajectory. We impose a strict condition on the recovery trajectory that the robot at P has the outmost orientation and the distance of the recovery trajectory is equal to s_{max} . If the recovery trajectory collides with an obstacle region, decrease s_t and go to (2). Otherwise, the viewpoint calculated in (2) is selected as the next one, and the calculated s_t and λ_t are used as the control input to move to the next viewpoint. Exit loop.

The feature of the proposed method is that the next viewpoint and the control input are determined on-line so that the safety of the robot motion is guaranteed by considering the worst case of uncertainty.

3.2.3 The need for the on-line viewpoint planning

By comparing the simulation results of the on-line and the off-line methods, we show that it is necessary to plan on-line. The target trajectory in the simulation is composed of a straight line whose total distance is 8[m] and s_{max} is set to 1[m]. Each variance is set as follows: $\sigma_s^2 = 0.1^2 * s_t/s_{max}[m^2]$, $\sigma_\lambda = 3[\text{deg}]$, and $\sigma_\phi = 0[\text{deg}]$. The pixel error caused by quantization is set to $\sigma_{x_l} = \sigma_{x_r} = 1[\text{pixel}]$. In the simulation, we add the 3σ Gaussian noise to each input to the robot.

In the case of the off-line method, we assume that the robot is always located at the predicted position be-

cause we cannot know a real position in advance[2]. Fig. 7 is a navigation result using the off-line planned viewpoints. Each arrow indicates a state of the robot, and its end point indicates the estimated position, which is not the same position as the planned viewpoint. The result shows that the robot often deviates from the target trajectory by actual errors, and that there is a possibility of collision.

Fig. 8 shows the result of the same simulation using the proposed on-line planning method. Even if the estimated position is different from the planned next viewpoint, the robot moves without collision because the planning is performed based on the estimated current position.

3.2.4 Non-stop motion

Since the visual processing requires much computation time, the result of the vision observation is ob-

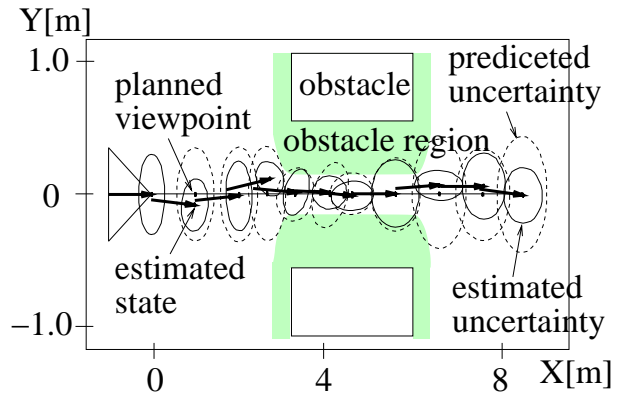


Fig. 7. Motion result using the off-line planned viewpoints.

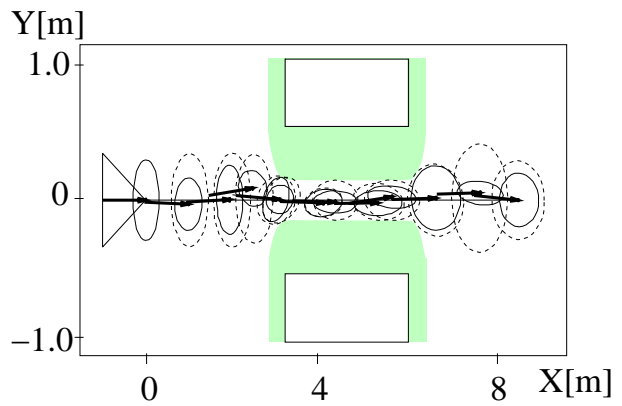


Fig. 8. Motion result using the on-line planning strategy.

tained with delay. For this problem, we utilize the non-stop navigation method[5,6]. In the method, the robot moves to a destination without stopping while it is processing the visual data. When the robot obtains the processing result later, it retroactively integrates the delayed sensory information into the state estimation. Since our robot is controlled by a single control input between two consecutive viewpoints, the current state and uncertainty can be retroactively estimated from the control input and the updated previous state and its uncertainty.

Fig. 9 illustrates the non-stop navigation strategy and the retroactively estimated states and uncertainties. Suppose the robot is located at $\hat{\mathbf{X}}_{t-1}$ with uncertainty e_1 . The robot inputs an image and then starts moving to the next viewpoint $\hat{\mathbf{X}}_t$ by a control input \mathbf{U}_{t-1} . The uncertainty at time t can be calculated from Eq. (3) and will be increased to e_2 due to the dead reckoning error. At time t , the robot obtains the result of observation at $t-1$, and then estimates the state $\bar{\mathbf{X}}_{t-1}$ and uncertainty e_3 using the Kalman filter (see Appendix A). With the state $\bar{\mathbf{X}}_{t-1}$ and the input \mathbf{U}_{t-1} , the robot can recalculate the current state $\hat{\mathbf{X}}_t$ and its uncertainty e_4 using Eqs. (1)(3), respectively.

Assuming that the time for one processing cycle including visual processing is constant, it is possible for the robot to move continuously by controlling the speed to be proportional to the distance to the next viewpoint. In this non-stop motion strategy, e_2 is the predicted uncertainty which is used to check the safety.

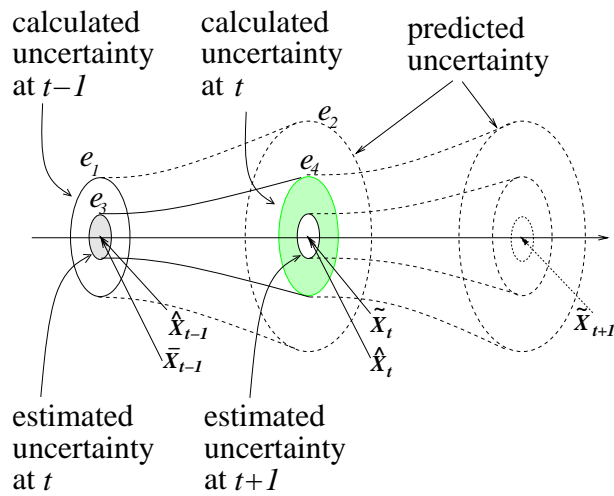


Fig. 9. Non-stop motion and estimated positional uncertainties.

3.3 Landmark planning

From the given landmark candidates, the robot selects a pair of landmarks which is the nearest and visible from the current robot position. If the robot cannot select a visible pair, it selects the nearest one.

The visibility is judged based on the stereo observation model (see Fig. 4). From Eq. (5), the projected position \mathbf{I} of a landmark in the stereo images is obtained as follows:

$$\mathbf{I} = \begin{bmatrix} x_l \\ x_r \end{bmatrix} = \begin{bmatrix} f \frac{c_x + a}{c_y} \\ f \frac{c_x - a}{c_y} \end{bmatrix}. \quad (11)$$

From Eq. (9), we can obtain the landmark position in the camera coordinates, $\mathbf{O} = [c_x \ c_y]^T$, as follows:

$$\mathbf{O} = \mathbf{R}^{-1} [(\theta + \phi) - \frac{\pi}{2}] [\mathbf{L} - \mathbf{X}]. \quad (12)$$

From Eqs. (11)(12), we can obtain the following non-linear equation

$$\mathbf{I} = \mathbf{J}(\mathbf{X}, \mathbf{L}). \quad (13)$$

Since we assume that the landmark position has no uncertainty, the projected uncertainty of the landmark in the image depends only on the robot uncertainty Σ . By linearizing Eq. (13), we obtain the covariance matrix of \mathbf{I} as follows:

$$\Sigma = \frac{\partial \mathbf{J}}{\partial \mathbf{X}} \Sigma \frac{\partial \mathbf{J}^T}{\partial \mathbf{X}}. \quad (14)$$

If the uncertainty area of a landmark is completely included in the image, the landmark is considered to be visible. Once the landmark is determined, the viewing direction is set to the center position of the pair or the landmark.

4 Landmark observation using stereo vision

There are many artificial objects including various vertical straight segments in a typical indoor environment. We use such vertical segments as landmarks, and the attribute of landmarks such as position, length and direction[9] is given.



Fig. 10. Result of landmark detection.

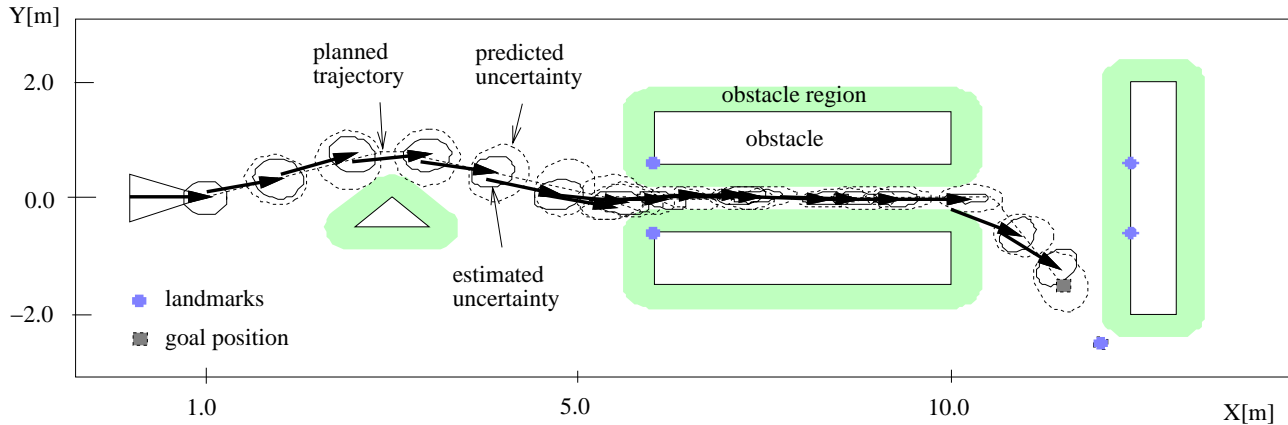


Fig. 11. Navigation result using the on-line planned viewpoints adapted to environment.

We can restrict a searching region for the given landmark to the predicted area in the image by Eqs. (13)(14). Inside the area, vertical line segments are extracted from edges obtained by applying a horizontal differential operator to the input image. To match segments in the stereo images, we calculate similarity which consists of overlapping ratio, and orientation and length similarity, and then dynamic programming method is applied to determine the best correspondence by comparing the similarity[11].

From results of the stereo matching, the segment positions on the X - Y plane is calculated by the stereo geometry. Then, by comparing the segment position to the given landmark we can select candidates for each landmark considering the positional uncertainty.

Given a pair of landmarks for localization, the robot generates a list of possible pairs of the observed landmark candidates, and utilizes each pair to estimate

its state. Among the pairs whose corresponding estimated positions are within the predicted positional uncertainty ellipse, the robot selects a pair which has the minimum distance between the estimated position and the predicted one. If a single landmark is given, the robot selects a segment which is the nearest to the predicted landmark position.

Fig. 10 is an observation result of the landmark pair; one is the right edge of the white board and the other is the left edge of the partition. The horizontal lines at the top and bottom of the image indicate the predicted position and its uncertainty of the landmarks, and the black vertical lines show the detected position of the landmarks.

5 Experiment

We conducted experiment using an actual mobile robot shown in Fig. 2. Each parameter is set to the same value as the one used in section 3.2.3.

Fig. 11 shows an experimental result in our laboratory. The total length of the target trajectory is about 13[m], and the trajectory is composed of lines and arcs. The outer and inner ellipses at each viewpoint denote the predicted and the estimated uncertainty of the robot position, respectively. The experimental result shows that the robot successfully reached the goal position without collision using the adaptively determined viewpoints; it moved quickly in wide open spaces but slowly in the narrow space.

Fig. 12 shows the time chart of processing. All kinds of processing is performed sequentially; one cycle of processing takes 3[sec]. The maximum speed of the robot is 0.33[m/sec]. Fig. 13 shows the results of the landmark detection, and Fig. 14 shows the movement of the robot.

6 Conclusion

In this paper, we have proposed an on-line viewpoint and motion planning method for a mobile robot to reach a goal position safely and quickly under uncertainty. Based on the uncertainties of vision and motion, the safety of a viewpoint is determined. To reduce the number of observations as much as possible, the method repeatedly selects the farthest *safe* position as the next viewpoint. The method works on-line to cope with actual errors in the robot movement. Experimental results show the validity of the

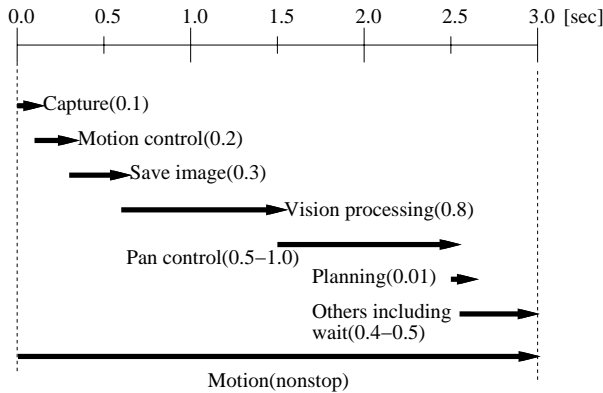


Fig. 12. Processing time chart.

proposed method.

However, this study utilized given landmarks in a relatively simple scene. Thus, we are now considering the problem of selecting useful landmarks autonomously from a more complicated scene. We are also planning to extend the method to cope with unknown obstacles.

Appendix

A Estimating state and covariance using the Extended Kalman Filter

Eq. (10) is a constraint equation in the case that the robot at state \mathbf{X}_t makes the observation \mathbf{O} of a given landmark \mathbf{L} . This equation is linearized by the first-order Taylor series expansion around the mean values, $\hat{\mathbf{X}}_t$, $\hat{\mathbf{O}}_t$, and $\hat{\mathbf{L}}$:

$$\begin{aligned} G(\mathbf{X}_t, \mathbf{O}_t, \mathbf{L}) &\approx G(\hat{\mathbf{X}}_t, \hat{\mathbf{O}}_t, \hat{\mathbf{L}}) + \frac{\partial G}{\partial \mathbf{X}_t}(\mathbf{X}_t - \hat{\mathbf{X}}_t) \\ &+ \frac{\partial G}{\partial \mathbf{O}_t}(\mathbf{O}_t - \hat{\mathbf{O}}_t) + \frac{\partial G}{\partial \mathbf{L}}(\mathbf{L} - \hat{\mathbf{L}}) = \mathbf{0}. \end{aligned} \quad (\text{A.1})$$

Since we assume that the given map including landmark information has no uncertainty, \mathbf{L} is always equal to $\hat{\mathbf{L}}$. Thus,

$$\begin{aligned} G(\hat{\mathbf{X}}_t, \hat{\mathbf{O}}_t, \mathbf{L}) &+ \frac{\partial G}{\partial \mathbf{X}_t}(\mathbf{X}_t - \hat{\mathbf{X}}_t) \\ &+ \frac{\partial G}{\partial \mathbf{O}_t}(\mathbf{O}_t - \hat{\mathbf{O}}_t) = \mathbf{0}. \end{aligned} \quad (\text{A.2})$$

Eq. (A.2) can be rewritten in a new linear equation form

$$\mathbf{Y}_t = \mathbf{H}_t \mathbf{X}_t + \mathbf{V}_t, \quad (\text{A.3})$$

where

$$\mathbf{Y}_t = -G(\hat{\mathbf{X}}_t, \hat{\mathbf{O}}_t, \mathbf{L}) + \frac{\partial G}{\partial \mathbf{X}_t} \hat{\mathbf{X}}_t,$$

$$\mathbf{H}_t = \frac{\partial G}{\partial \mathbf{X}_t},$$

$$\mathbf{V}_t = \frac{\partial G}{\partial \mathbf{O}_t}(\mathbf{O}_t - \hat{\mathbf{O}}_t).$$

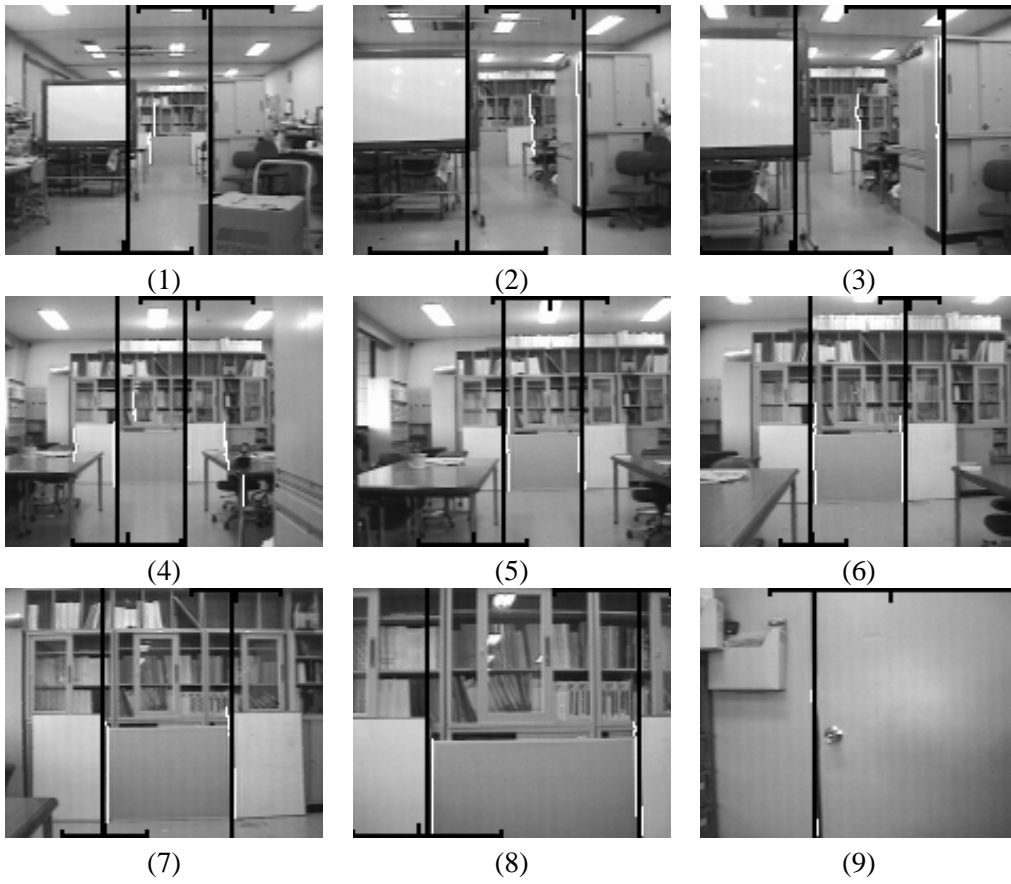


Fig. 13. Observed landmarks.

In Eq. (A.3) \mathbf{Y}_t is the new observation, \mathbf{H}_t is the linear transformation, and \mathbf{V}_t is the random observation error. The covariance matrix of the observation, Σ_t , is obtained as follows:

$$\Sigma_t = E[\mathbf{V}_t \mathbf{V}_t^T] = \frac{\partial \mathbf{G}}{\partial \mathbf{O}_t} \Sigma_t \frac{\partial \mathbf{G}^T}{\partial \mathbf{O}_t}. \quad (\text{A.4})$$

We can see that the observation uncertainty for the given landmark includes the stereo observation uncertainty Σ_t in Eq. (8). Based on the observation \mathbf{Y}_t and its uncertainty Σ_t , the state and uncertainty of the robot can be estimated and updated using the Kalman Filter.

The Kalman Filter consists of the following equations[10]:

$$\bar{\mathbf{X}}_t = \hat{\mathbf{X}}_t + \mathbf{K}_t [\mathbf{Y}_t - \mathbf{H}_t \hat{\mathbf{X}}_t], \quad (\text{A.5})$$

$$\Sigma_{\bar{\mathbf{X}}_t} = [\mathbf{I} - \mathbf{K}_t \mathbf{H}_t] \Sigma_{\hat{\mathbf{X}}_t}, \quad (\text{A.6})$$

$$\mathbf{K}_t = \Sigma_{\hat{\mathbf{X}}_t} \mathbf{H}_t^T [\mathbf{H}_t \Sigma_{\hat{\mathbf{X}}_t} \mathbf{H}_t^T + \Sigma_t]^{-1}, \quad (\text{A.7})$$

where $\bar{\mathbf{X}}_t$ and $\Sigma_{\bar{\mathbf{X}}_t}$ denote the estimated state and covariance matrix, and $\hat{\mathbf{X}}_t$ and $\Sigma_{\hat{\mathbf{X}}_t}$ denote the predicted state and covariance matrix calculated in Eqs. (1)(3) at time t-1, respectively. \mathbf{K}_t is called the Kalman gain.

References

- [1] J. Miura and Y. Shirai, Vision and Motion Planning for a Mobile Robot under Uncertainty, *The Int. Journal of Robotics Research* 16 (6) (1997) 806–825.
- [2] I.H. Moon, J. Miura, Y. Yanagi, and Y. Shirai, Planning of Vision-Based Navigation for a Mobile Robot under Uncertainty, *Proc. of IEEE/RSJ Int. Conf. on Intelligent Robots and Systems* (1997) 1202–1207.
- [3] N. Ayache and O.D. Faugeras, Maintaining Representations of the Environment of a Mobile

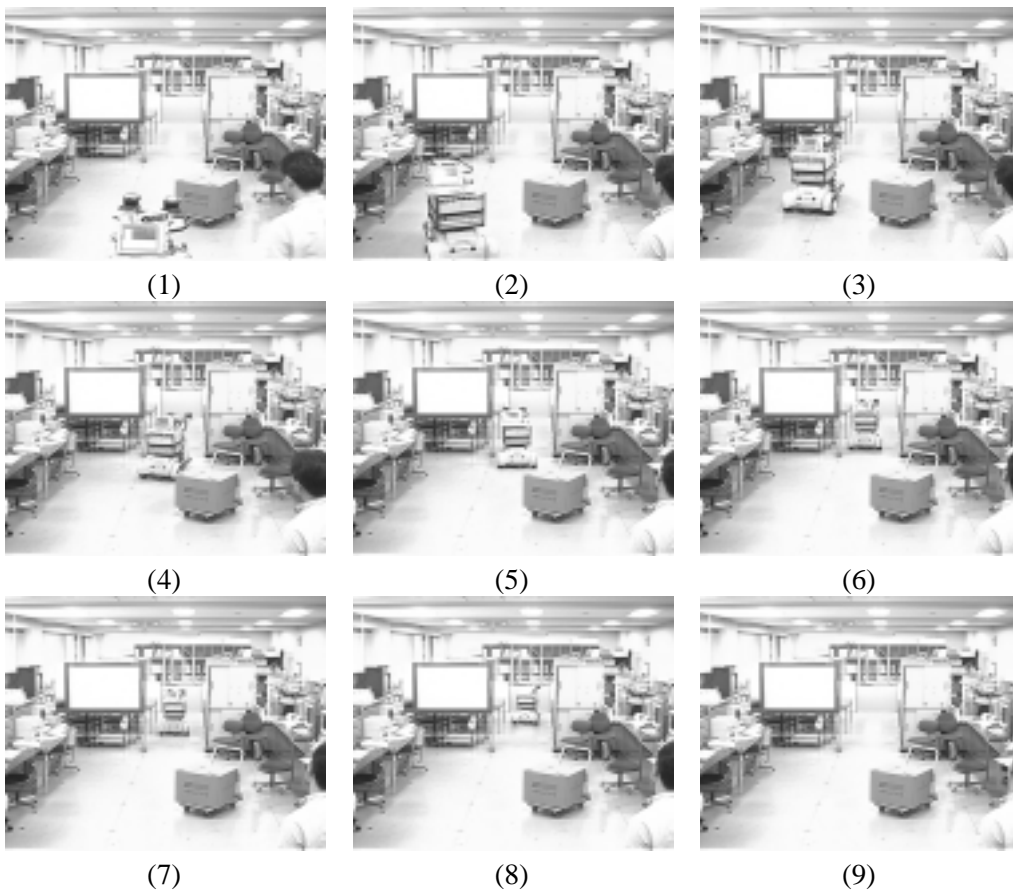


Fig. 14. Mobile robot motion.

- Robot, *IEEE Trans. on Robotics and Automation* 5 (6) (1989) 804–819.
- [4] D.J. Kriegman, E. Triendl, and T.O. Binford, Stereo Vision and Navigation in Buildings for Mobile Robots, *IEEE Trans. on Robotics and Automation* 5 (6) (1989) 792–803.
- [5] A. Kosaka, M. Meng, and A. Kak, Vision Guided Mobile Robot Using Retroactive Updating of Position Uncertainty, *Proc. of IEEE Int. Conf. on Robotics and Automation* (1993) 1–7.
- [6] S. Maeyama, A. Ohya, and S. Yuta, Non-Stop Outdoor Navigation of a Mobile Robot, *Proc. of IEEE/RSJ Int. Conf. on Intelligent Robots and Systems* (1995) 130–135.
- [7] K. Komoriya, E. Oyama, and K. Tani, Planning of Landmark Measurement for the Navigation of a Mobile Robot, *Proc. of IEEE/RSJ Int. Conf. on Intelligent Robots and Systems* (1992) 1476–1481.
- [8] K. Nagatani and S. Yuta, Path and Sensing Point Planning for Mobile Robot Navigation to Minimize the Risk of Collision, *Proc. of IEEE/RSJ Int. Conf. on Intelligent Robots and Systems* (1993) 2198–2203.
- [9] J. Miura and Y. Shirai, An Uncertainty Model of Stereo Vision and Its Application to Vision-Motion Planning of Robot, *Proc. 13th Int. Joint Conf. on Artificial Intelligence* (1993) 1618–1623.
- [10] P.S. Maybeck, The Kalman Filter: An Introduction to Concepts, in: I.J. Cox and G.T. Wilfong, eds., *Autonomous Robot Vehicles*, Springer-Verlag (1990) 194–204.
- [11] S.H. Lee and J.J. Leou, A Dynamic Programming Approach to Line Segment Matching in Stereo Vision, *Pattern Recognition* 28 (8) (1994) 961–986.